

## Lattice and Thermal Misfit Dislocations in Epitaxial $\text{CaF}_2/\text{Si}(111)$ and $\text{BaF}_2\text{-CaF}_2/\text{Si}(111)$ Structures

S. Blunier, H. Zogg, C. Maissen, and A. N. Tiwari

*AFIF (Arbeitsgemeinschaft für industrielle Forschung) at Swiss Federal Institute of Technology, ETH Hönggerberg, CH-8093 Zürich, Switzerland*

R. M. Overney and H. Haefke

*Institute of Physics, University of Basel, CH-4056 Basel, Switzerland*

P. A. Buffat

*Institute for Electron Microscopy, Swiss Federal Institute of Technology EPFL, CH-1015 Lausanne, Switzerland*

G. Kostorz

*Institute of Applied Physics, Swiss Federal Institute of Technology, ETH Hönggerberg, CH-8093 Zürich, Switzerland*  
(Received 4 February 1992)

Atomic force microscopy reveals straight slip steps resulting from dislocation glide in the primary  $\{100\}\langle 110\rangle$  glide system in "low mismatch"  $\text{CaF}_2/\text{Si}(111)$  structures. From the height and spacing of the steps, the strain relieved by these misfit dislocations is compatible with the relief of the tensile thermal strain change on cooldown. In "high mismatch"  $\text{BaF}_2/\text{CaF}_2/\text{Si}(111)$  structures, dislocations which relieve the thermal mismatch change are mobile, while the 14% lattice mismatch is mainly overcome by sessile misfit dislocations with Burgers vectors parallel to the interface.

PACS numbers: 68.55.Bd, 68.55.Jk, 68.60.Bs

Group-IIA-fluoride thin films grown epitaxially onto Si have initially attracted attention for potential device applications [1], as buffer layers for overgrowth with different semiconductor films [1,2], and because of interesting structural and electronic properties of the ionic/covalent interface [3-5]. At room temperature (RT), the lattice constant of  $\text{CaF}_2$  is only 0.6% higher than that of Si, while that of  $\text{BaF}_2$  is 14% higher. However, the thermal expansion coefficients of the IIA fluorides are about 7 times larger than in Si. The lattice mismatch between  $\text{CaF}_2$  and Si is therefore as high as 2.4% at 750°C, a typical growth temperature in molecular beam epitaxy (MBE). Growth is layer by layer on (111)-oriented Si substrates, and the lattice orientation is type *B* with respect to the substrate. After the layer thickness exceeds the critical coherency thickness  $h_c$  ( $\approx 3$  nm), the lattice strain starts to relax during growth owing to the formation of misfit dislocations [6], and decreases to very small values for films thicker than about 50 nm. In such films, a 1.8% tensile strain is therefore expected at RT as a result of the thermal expansion mismatch if no plasticity occurs after growth. A thermally caused strain of this type is found, e.g., in  $\text{CoSi}_2$  on Si(111) [7] or in GaAs on Si [8]. However, in  $\text{CaF}_2$  on Si(111) [9] or stacks of  $\text{BaF}_2\text{-CaF}_2$  on Si(111) [10], it was found that the observed tensile strain at RT decreases to near zero with increasing layer thickness. Therefore, plastic relaxation occurs even *after* growth during cooldown.

Although the fluorides are rather brittle, dislocation movement in bulk  $\text{CaF}_2$  single crystals ( $\text{CaF}_2$  is harder than  $\text{BaF}_2$ ) has been studied between 100°C and RT

[11]. The dislocations move at speeds from 0.1 to 100  $\mu\text{m}/\text{sec}$  under resolved shear stresses of 1 to 100 MPa (corresponding to shear strains of order  $10^{-4}$  to  $10^{-2}$ ). These are velocities which are more than sufficient for strain relaxation, even for fast temperature changes, at least as long as potential glide planes are sufficiently inclined to the film plane. However, impurities reduce the velocities [11].

The microscopic understanding of misfit dislocation mechanisms in systems with the diamond or sphalerite structure such as SiGe/Ge [12] or GaInAs/GaAs [13] is quite advanced: In (001)-oriented systems with "low mismatch" (1%-2%), 60° dislocations with inclined Burgers vectors move on (111) glide planes to the interface where they contribute to the strain relief. The misfit dislocations form either by bending of threading dislocations or by nucleation of half loops at defects inside the material [14] or at the free surface [13]. In "high mismatch" systems where initial growth is by islands (mismatch 2%-4%), 90° sessile (edge) dislocations with the Burgers vector parallel to the interface dominate; they are formed, e.g., by interaction of two glissile 60° dislocations.

The primary glide system in IIA fluorides is  $\{100\}\langle 110\rangle$ , and secondary glide is on  $\{110\}$  planes [11]. Glide on  $\{111\}$  planes has been reported by one author only [15]. The (111) interface plane is therefore not an easy glide plane, and strain relieving dislocations of the primary  $\{100\}$  glide system must have Burgers vectors inclined to the interface.

In the following, we will describe the strain relief in low mismatch  $\text{CaF}_2$  on Si(111) and in high mismatch

BaF<sub>2</sub>/CaF<sub>2</sub> on Si(111) systems. We will show that in both systems the *thermal* mismatch strain is relieved by glide of dislocations in the primary glide system, while sessile dislocations are mainly responsible for relieving the *lattice* mismatch strain at growth temperature in the high mismatch system.

Published transmission electron microscopy (TEM) studies concern the structural properties of the CaF<sub>2</sub>/Si(111) interface and the influence of surface steps in the substrate [4,16], but not the plasticity of fluoride layers on silicon. TEM is rather difficult to perform owing to the difficult preparation of cross sections and the instabilities of fluorides upon electron irradiation.

We chose atomic force microscopy (AFM) [17] for most of the work to directly image the insulating fluoride surfaces. To date, no AFM studies are known with epitaxial or bulk fluorides. Scanning tunneling microscopy (STM) was used to investigate the initial stages of CaF<sub>2</sub> nucleation on Si [18]; however, thicker layers have to be investigated with AFM because of the insulating nature of the fluorides. We used a commercial instrument with integrated Si<sub>3</sub>N<sub>4</sub> tips, and 0.12-N/m spring constants. The applied force was of order 10 nN. The images presented here are unfiltered, raw data. All measurements were performed in air.

Figure 1 shows an AFM image of a 180-nm-thick epitaxial CaF<sub>2</sub> layer on Si(111). The substrate was cleaned with a Shiraki procedure, and the layer was grown by MBE at about 750°C substrate temperature [19]. The substrate surface is (111) oriented within better than 0.5°.

The most striking features in the figure are the three sets of parallel straight steps with 60° angles between each set. The line directions correspond to  $\langle\bar{1}10\rangle$  directions of the sample, i.e., to the intersections of the {100} glide planes with the (111) surface (see Fig. 2). We did not observe such lines with AFM on bulk fluorides, and cleavage steps in bulk materials have very different morphologies. A height profile is shown along the marked line in Fig. 1(b). Within the statistical accuracies, all step heights can be explained by multiples of  $a/\sqrt{3}$  ( $a$  is the lattice constant), i.e., to the spacings of (111)-oriented triple F<sup>-</sup>-Ca<sup>++</sup>-F<sup>-</sup> atomic layers. This corresponds to multiples of the perpendicular projection  $b_{\perp}$  of the  $(a/2)\langle 110\rangle$  Burgers vectors. The heights are consistent with the interpretation that the surface steps are due to glide of one or a few dislocations along an individual {100} glide plane. As a result of the threefold symmetry, the steps lead to triangular terraces with altitude differences corresponding to these step heights. In Fig. 1, steps corresponding to  $nb_{\perp}$  with  $n=1, 2, \text{ or } 3$  are visible in different grey tones. We did not observe steps with  $n \geq 4$ . Careful analysis of different images yielded the number of observable traces and their corresponding step heights  $n$ .

For the three equivalent {001}⟨110⟩ glide systems with

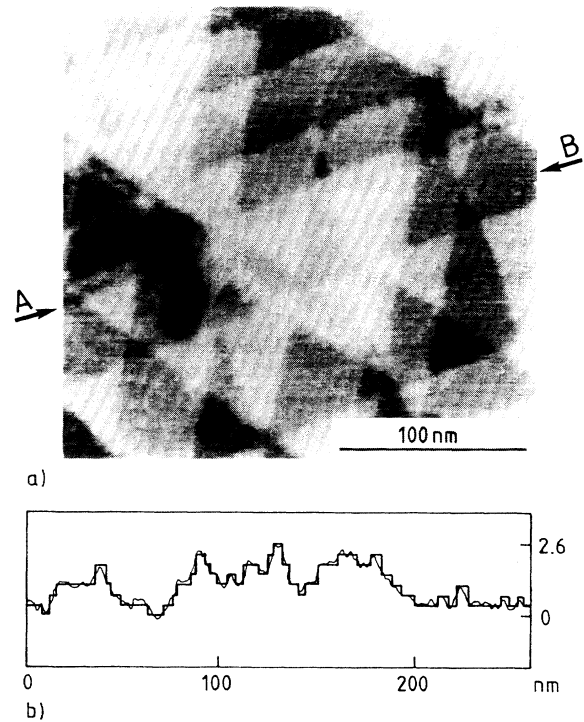


FIG. 1. (a) AFM image of a 180-nm-thick epitaxial CaF<sub>2</sub> layer on Si(111). The straight slip steps are parallel to the three  $\langle\bar{1}10\rangle$  directions. The offsets in height of the triangles within the slip step lines are multiples of the projection of the Burgers vectors, as indicated in (b) the height profile along the line A-B.

Burgers vector  $b$  inclined by an angle  $\Theta$  with respect to the interface normal, the spacing  $s$  between individual dislocations (i.e., slip steps normalized to  $n=1$ ) required to relieve a misfit strain  $\epsilon$  is given by elementary geometrical considerations as

$$s = \frac{3}{2} \sin\Theta b / \epsilon.$$

Using this formula, the experimentally observed spacing corresponds to a misfit relief of  $1.7\% \pm 0.3\%$ . This fits well with the strain change  $\epsilon_{\text{thermal}} = 1.8\%$  on cooldown from growth temperature (750°C) to RT.

A likely model of misfit relaxation is therefore that most of the misfit dislocations are glissile on inclined {100} planes and have formed, e.g., by nucleation of half loops *during* growth because of the lattice mismatch, or *after* growth on cooldown to room temperature as a consequence of the thermal expansion mismatch (which leads to a slight tensile strain at RT). The nucleation of half loops at the surface is energetically favorable over other mechanisms [13], e.g., nucleation within the layer. Misfit dislocations with Burgers vectors parallel to the interface plane, caused, e.g., by atomic steps in the substrate [16], or by shift of interfacial Ca atoms from the  $H_3$  to the  $T_4$  site (or vice versa) as proposed in Ref. [5]

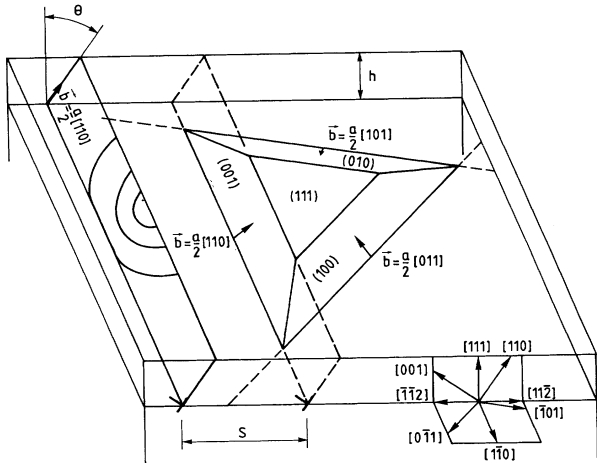


FIG. 2. Schematic drawing of dislocation nucleation and glide in the primary  $\{100\}\langle 110\rangle$  system for (111)-oriented films.

may be present too. However, these dislocations are not visible as slip steps at the surface. The same may be true for glissile dislocations of the primary slip system which form during growth because the slip step they leave behind at the surface may be smeared out by the condensation of further arriving atoms when the layer thickness increases [during growth, most of the strain relaxes within  $(2-3)h_c$ ]. AFM images of thinner films exhibit an increased dislocation density which include steps from glissile dislocations which formed during growth.

We therefore state that for  $\text{CaF}_2$  on  $\text{Si}(111)$  the lattice mismatch during growth is, like the thermal mismatch, overcome by inclined glissile dislocations rather than by dislocations with Burgers vectors parallel to the interface. This is because the latter have to climb to the interface, while glide on the primary slip system is very easy. For the relaxation of the mismatch, the system prefers dislocations acting in the primary glide system with inclined  $\langle 110\rangle$  Burgers vectors although such dislocations do not relieve as much strain as dislocations with Burgers vectors parallel to the interface. In some early work on epitaxial  $\text{CaF}_2$  on  $\text{Si}$ , it was reported that the layers are cracked [1], while we do not observe any cracks in high-quality films. Cracks can form if too many obstacles resulting from contamination or structural defects hinder dislocation glide.

Figure 3 shows a similar AFM image of a 190-nm-thick  $\text{BaF}_2$  layer grown on  $\text{CaF}_2/\text{Si}(111)$ . The intermediate  $\text{CaF}_2$ , which is needed for compatibility to obtain high-quality untwinned  $\text{BaF}_2$ , was about 60 nm thick. In addition to the curved growth steps due to variations of the layer thickness, the micrograph again shows the same three sets of  $\{100\}\langle 110\rangle$ -type glide step traces as in Fig. 1. Despite the quality of the image being somewhat inferior, the observable step spacing is certainly too wide to explain the  $\approx 16\%$  lattice and thermal expansion mismatch of  $\text{BaF}_2$  grown at  $750^\circ\text{C}$  on  $\text{Si}$ . However, the spacing is

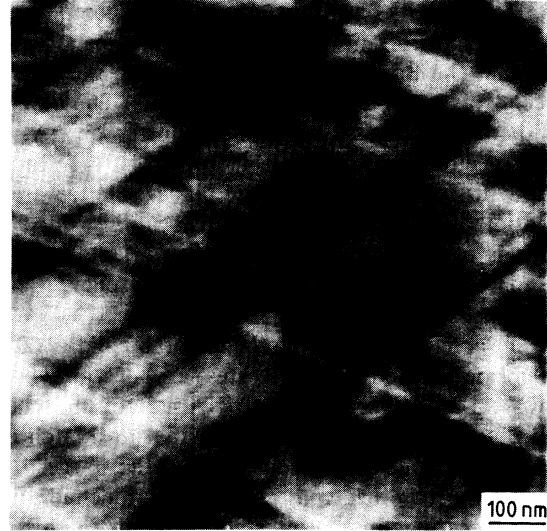


FIG. 3. AFM image of a  $\text{BaF}_2/\text{CaF}_2$  stack on  $\text{Si}(111)$ . The spacing of slip steps is much wider than would be required to account for  $> 14\%$  lattice mismatch.

consistent with the relaxation of the thermal mismatch alone.

Since we know that the total strain in the  $\text{BaF}_2$  is also almost completely relaxed, some other strain-relieving dislocations must be active for relaxation of most of the  $16\%$  lattice mismatch at growth temperature. Figure 4 shows a cross-section high-resolution TEM picture of the  $\text{CaF}_2/\text{BaF}_2$  interface of a stack grown on  $\text{Si}$ . The lattice orientation of  $\text{BaF}_2$  and  $\text{CaF}_2$  is the same. The spacing of the visible  $\text{F}^- - \text{X}^{++} - \text{F}^-$  ( $\text{X} = \text{Ca}$  or  $\text{Ba}$ ) triple layers is about  $14\%$  larger in  $\text{BaF}_2$  than in  $\text{CaF}_2$ . This  $14\%$  mismatch is overcome by a wall of dislocations lying in the  $\text{CaF}_2/\text{BaF}_2$  interface with the dislocation lines spaced approximately every seventh layer as marked in the figure. Despite the fact that the quality of the image is not optimal, it is possible to draw Burgers circuits if they are drawn with sufficient distance from the dislocation

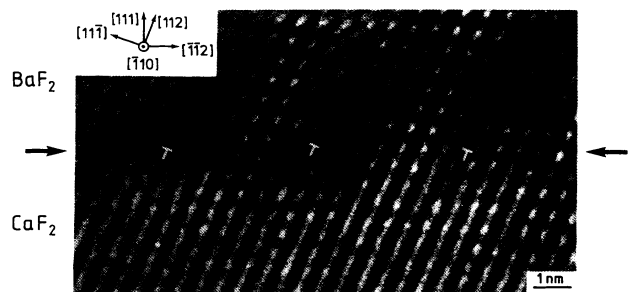


FIG. 4. High-resolution cross-section TEM image of a  $\text{BaF}_2/\text{CaF}_2$  interface. The extra half planes of the lattice misfit dislocations are marked. The dislocation lines are perpendicular to the micrograph, and the Burgers vectors lie in the interface plane.

cores. The circuits reveal that the in-plane components of the Burgers vectors lie along the  $(\bar{1}\bar{1}2)$  direction, which means that the Burgers vector is parallel to the (111) interface. This is not a primary glide plane. These dislocations therefore seem to be sessile. Most probably, their Burgers vectors are  $(a/2)[10\bar{1}]$  or  $(a/2)[01\bar{1}]$  (inclined  $\pm 30^\circ$  with respect to the image plane). These are  $60^\circ$  dislocations. Splitting of these dislocations into  $\langle 112 \rangle$  partials is unlikely because the lattice orientation is the same for  $\text{CaF}_2$  and  $\text{BaF}_2$ , and because of energetic considerations.

We observe a very similar behavior of glide traces if the fluoride-covered Si substrates are overgrown with narrow-gap IV-VI semiconductors used for thermal infrared detector arrays [2]: The thermal mismatch is relieved by gliding dislocations, while the large lattice mismatch must be overcome by another mechanism like sessile dislocations in the interface. Details of this work will be reported elsewhere.

In summary, we have been able to explain microscopically the lattice and thermal mismatch strain relief in epitaxial IIA fluorides on Si(111) substrates. For the low mismatch  $\text{CaF}_2/\text{Si}(111)$  system, we state that the lattice and thermal mismatch strains relieve down to room temperature mainly by glide of dislocations on  $\{100\}$  planes. The dislocations most probably nucleate in half loops at the surface, become misfit dislocations after glide down, and leave a surface step behind. For the high mismatch  $\text{BaF}_2\text{-CaF}_2/\text{Si}$  system, the thermal mismatch relaxation is the same as for the  $\text{CaF}_2/\text{Si}$  system, but the lattice mismatch is mainly overcome by sessile  $60^\circ$  dislocations located at the  $\text{CaF}_2/\text{BaF}_2$  interface with Burgers vectors parallel to the interface plane. Since these latter dislocations form already after growth of about one monolayer of  $\text{BaF}_2$ , it is easily understandable that there is no need for them to be glissile, and that their Burgers vectors are arranged in order to relieve a maximum of strain.

The financial support by the Swiss National Science Foundation is gratefully acknowledged.

- [1] For a review see L. J. Schowalter, and R. W. Fathauer, *CRC Crit. Rev. Solid State Mater. Sci.* **15**, 367 (1989).
- [2] H. Zogg and M. Hüppi, *Appl. Phys. Lett.* **47**, 133 (1985); H. Zogg, S. Blunier, T. Hoshino, C. Maissen, J. Masek, and A. N. Tiwari, *IEEE Trans. Electron Dev.* **38**, 1110 (1991).
- [3] R. M. Tromp and M. C. Reuter, *Phys. Rev. Lett.* **61**, 1756 (1988).
- [4] J. L. Batstone, J. M. Phillips, and E. C. Hunke, *Phys. Rev. Lett.* **60**, 1394 (1988); **61**, 2274 (1988).
- [5] J. Zegenhagen and J. R. Patel, *Phys. Rev. B* **41**, 5315 (1990).
- [6] For a recent review see E. A. Fitzgerald, *Mater. Sci. Rep.* **7**, 87 (1991).
- [7] G. Bai, M.-A. Nicolet, T. Vreeland, Jr., Q. Ye, and K. L. Wang, *Appl. Phys. Lett.* **55**, 1874 (1989).
- [8] R. M. Lum, J. K. Klingert, R. B. Bylisma, A. M. Glass, A. T. Macrander, T. D. Harris, and M. G. Lamont, *J. Appl. Phys.* **64**, 6727 (1988).
- [9] S. Hashimoto, J.-L. Peng, W. M. Gibson, L. J. Schowalter, and R. W. Fathauer, *Appl. Phys. Lett.* **47**, 1071 (1985).
- [10] H. Zogg, *Appl. Phys. Lett.* **49**, 933 (1986).
- [11] R. N. Katz and R. L. Coble, *J. Appl. Phys.* **45**, 2382 (1974).
- [12] E. P. Kvam, D. M. Maher, and C. J. Humphreys, *J. Mater. Res.* **5**, 1900 (1990).
- [13] S. Sharan and J. Narayan, *J. Appl. Phys.* **66**, 2376 (1989). (*InGaAs/GaAs*)
- [14] D. J. Easlesham, D. M. Maher, E. P. Kvam, J. C. Bean, and C. J. Humphreys, *Phys. Rev. Lett.* **62**, 187 (1989).
- [15] C. C. Desai, *Surf. Technol.* **14**, 353 (1981).
- [16] F. A. Ponce, G. B. Anderson, M. A. O'Keefe, and L. J. Schowalter, *J. Vac. Sci. Technol. B* **4**, 1121 (1986); L. J. Schowalter, R. W. Fathauer, F. A. Ponce, G. Anderson, S. Hashimoto, *Mater. Res. Soc. Symp. Proc.* **67**, 125 (1986).
- [17] G. Binnig, C. F. Quate, and C. Gerber, *Phys. Rev. Lett.* **56**, 930 (1986).
- [18] R. Wolkow and Ph. Avouris, *J. Microsc.* **152**, 167 (1988).
- [19] H. Zogg, S. Blunier, and J. Masek, *J. Electrochem. Soc.* **136**, 779 (1989).

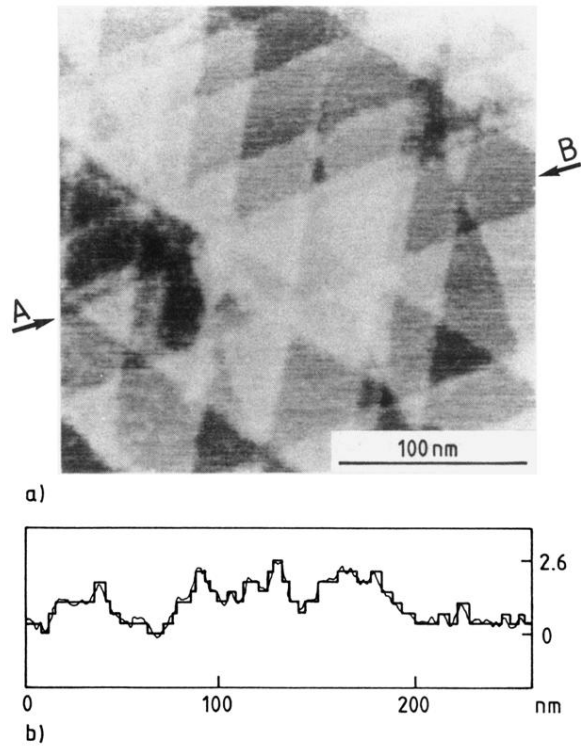
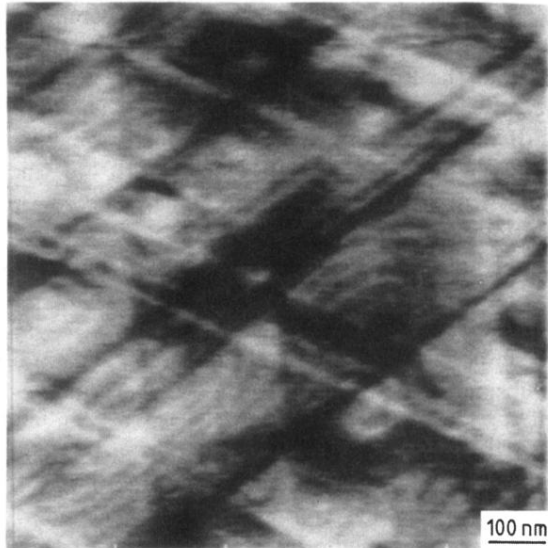


FIG. 1. (a) AFM image of a 180-nm-thick epitaxial CaF<sub>2</sub> layer on Si(111). The straight slip steps are parallel to the three  $\langle \bar{1}10 \rangle$  directions. The offsets in height of the triangles within the slip step lines are multiples of the projection of the Burgers vectors, as indicated in (b) the height profile along the line *A-B*.



**FIG. 3.** AFM image of a  $\text{BaF}_2/\text{CaF}_2$  stack on  $\text{Si}(111)$ . The spacing of slip steps is much wider than would be required to account for  $> 14\%$  lattice mismatch.

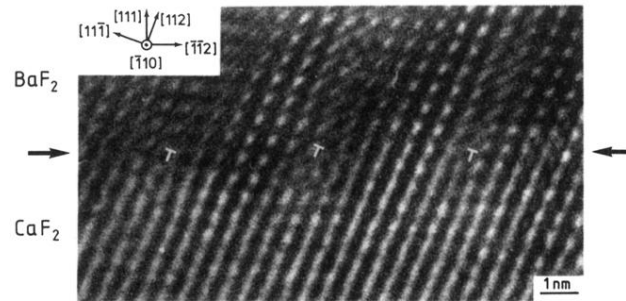


FIG. 4. High-resolution cross-section TEM image of a BaF<sub>2</sub>/CaF<sub>2</sub> interface. The extra half planes of the lattice misfit dislocations are marked. The dislocation lines are perpendicular to the micrograph, and the Burgers vectors lie in the interface plane.